

MULTI-OBJECTIVE GENETIC OPTIMIZATION OF SINGLE SHOT ULTRAFAST ELECTRON DIFFRACTION BEAMLINES

C. Gulliford, A. Bartnik, J. Maxson, I. Bazarov, Cornell University, NY 14853 USA

Abstract

We present the results of multiobjective genetic algorithm optimizations of two single-shot ultrafast electron diffraction beamlines: the first utilizes a 225 kV dc gun with a novel cryocooled photocathode system, while the second features a 100 MV/m 1.6-cell normal conducting rf (NCRF) gun. Both systems make use of a separate bunching cavity for longitudinal compression via velocity bunching situated between two focusing solenoids. In the case of the NCRF gun, a nine-cell $2\pi/3$ NCRF cavity is used for velocity bunching. Optimizations of the transverse projected emittance and coherence length as a function of bunch charge are presented and discussed in terms of the scaling laws derived in the charge saturation limit.

INTRODUCTION

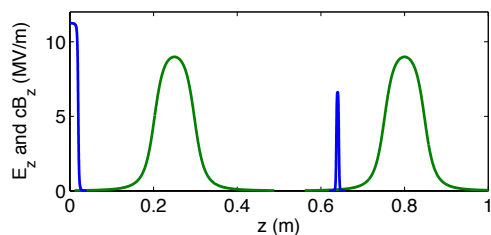
The study of biological samples, such as proteins, remains a challenge for single-shot ultrafast electron diffraction (UED) experiments, as they require large transverse coherence $L_{c,x} \geq 1$ nm, high bunch charges $q \geq 10^5 - 10^6$ electrons, and short pulse lengths $FW \leq 100$ fs [1, 2]. Designing a photoemission source for these bunch charges and beam sizes implies transporting a strongly space charge dominated beam [1–3]. Building on the successful application of multiobjective genetic algorithm (MOGA) optimized simulations of space charge dominated beams used in the design and operation of the Cornell photoinjector [4–6], we apply the same techniques to two similar UED beamlines: the first is a moderate energy dc gun followed by two solenoids sandwiching a NCRF buncher cavity [7–9], and the second is a 100 MV/m 2.856 GHz 1.6-cell NCRF gun followed by a nine-cell, $2\pi/3$ buncher cavity, sandwiched between two solenoids. In both cases the smallest MTEs considered achievable given the typical vacuum environment provided by each gun technology. In particular, recent work points to the ability to reduce the cathode MTE via cooling of the cathode [10], and data suggests cathode MTEs as low as 5 meV (cathode emittance of 0.1 $\mu\text{m}/\text{mm}$) may be possible using multiakali antimonide cathodes cooled to 20 K in a dc gun. For the NCRF gun a mean transverse energy (MTE) of 35 meV for the simulated photoelectrons is used, a value considered achievable through the use of multialkali photocathodes operated near threshold [11].

Figures 1 and 2 display the on-axis electric and magnetic fields for both beamlines. The buncher fields in the cryogun beamline make use of the 3 GHz Eindhoven design [7]. For the NCRF beamline buncher model, the dimensions of the first cell in the SLAC linac [12] were repeated a total of 9 times, to make a nine-cell $2\pi/3$ traveling wave buncher cavity. The field maps were generated in Poisson Superfish.

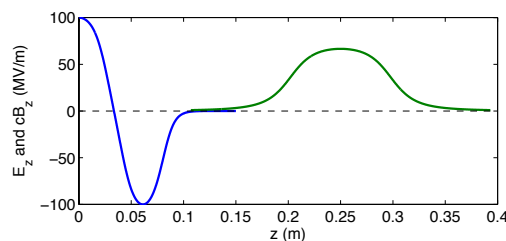
In both beamline examples, an analytic expression is used for the solenoid field maps:

$$B_z(z) = B_0 \left(\frac{\Delta z_+}{\sqrt{\Delta z_+^2 + R^2}} - \frac{\Delta z_-}{\sqrt{\Delta z_-^2 + R^2}} \right), \quad (1)$$

where $\Delta z_{\pm} = z \pm L/2$ and fit this model to solenoid field map data [13–15]. The fields used in space charge simulations are computed from the third order off-axis expansion of Eq. (1) in the radial offset r in a custom field element for the space charge code General Particle Tracer (GPT).



(a) Cryogun beamline.



(b) NCRF gun beamline.

Figure 1: On axis electric (blue) and magnetic (green) fields for the cryogun beamline (top) and NCRF gun beamline (bottom).

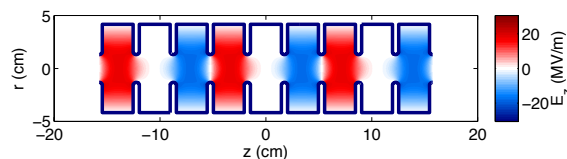


Figure 2: Electric fields for the 9 cell $2\pi/3$ bunching cavity used in the NCRF gun beamline.

RESULTS

Cryogun

For this set-up we first optimize the emittance as a function of bunch charge for a final bunch length of $\sigma_t \geq 500$ fs and two final transverse beam sizes $\sigma_x \leq 1000$ and $25 \mu\text{m}$, as shown in Figure 3. For the larger final spot size we note the $q_f^{2/3}$ scaling as predicted in [15]. Using these results as a seed for the optimization, we then optimized the coherence length as a function of bunch length for several different sample sizes. Figure 4 shows the resulting optimal coherence length as a function of final bunch length σ_t for each bunch charge and sample radius. For $q_f \geq 10^5$ electrons, the cryogun beam line provides solutions with $\sigma_t \leq 100$ fs for all three pinhole sizes. Computing the relative coherence length ($L_{c,x}/\sigma_x$) for a final bunch length of $\sigma_t \approx 100$ fs using the data from the fits to the optimization results (solid lines) and the fact that the beam size is well approximated as $\sigma_x \approx R/2$, gives $L_{c,x}/\sigma_x = 0.27 \text{ nm}/\mu\text{m}$. Increasing the required final charge to $q_f \leq 10^6$ electrons produces more varied coherence performance. For final spot sizes of $\sigma_x \geq 50 \mu\text{m}$ and final bunch lengths of $\sigma_t \approx 200$ fs, the cryogun beam line produces a relative coherence length of $0.11 \text{ nm}/\mu\text{m}$. For these parameters, estimating the relative coherence length gives $0.1 \text{ nm}/\mu\text{m}$ for a final $\sigma_t \leq 100$ fs.

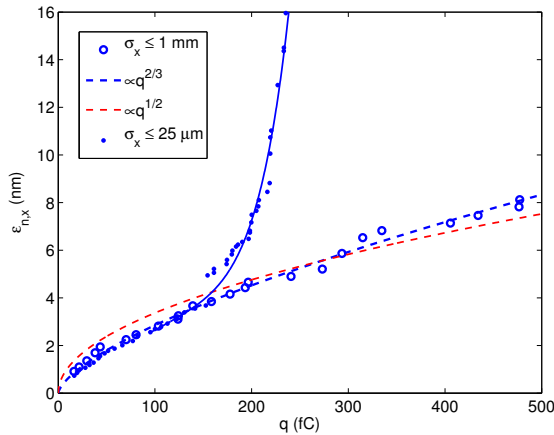
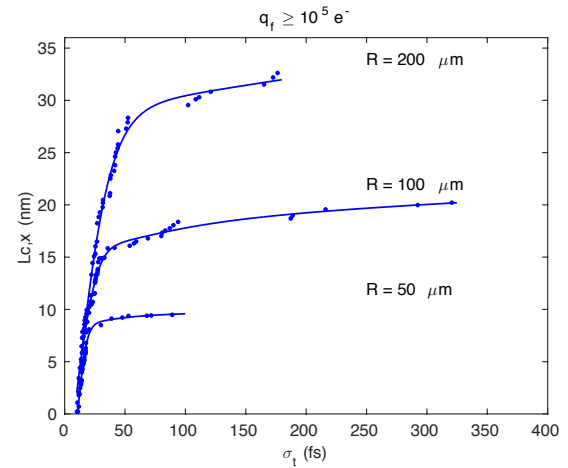


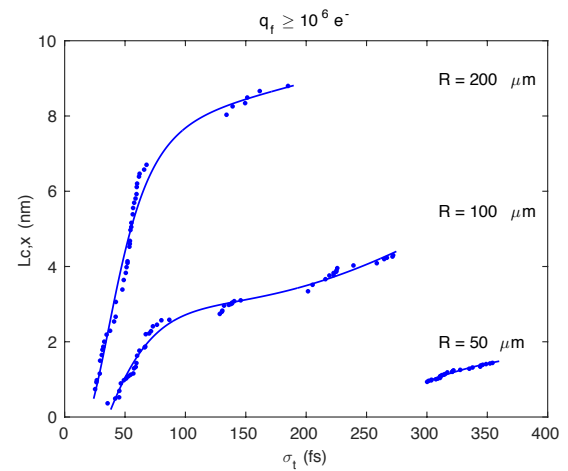
Figure 3: Optimized emittance as a function of bunch charge for the cryogun beamline.

NCRF Gun

As with the cryogun, we performed an initial round of emittance optimizations for a long final beam $\sigma_t \leq 500$ fs while constraining the transverse spot size: $\sigma_x \leq 25 \mu\text{m}$, and simultaneously maximizing the bunch charge. In these optimizations, we require that no particles are lost in beam transport (a simplification from the cryogun optimizations). Figure 5 shows the emittance performance and suggests that the emittance at the sample scales as $q^{2/3}$. Using the emittance vs bunch length solutions for a final spot size of $25 \mu\text{m}$ in Figure 5 as a seed, optimizations for the maximum transverse coherence length were performed. Figure



(a) Cryogun beamline with at least 10^5 electrons per bunch.



(b) Cryogun beamline with at least 10^6 electrons per bunch.

Figure 4: Optimized coherence length in the cryogun beamline for 10^5 (top) and 10^6 (bottom) electrons respectively.

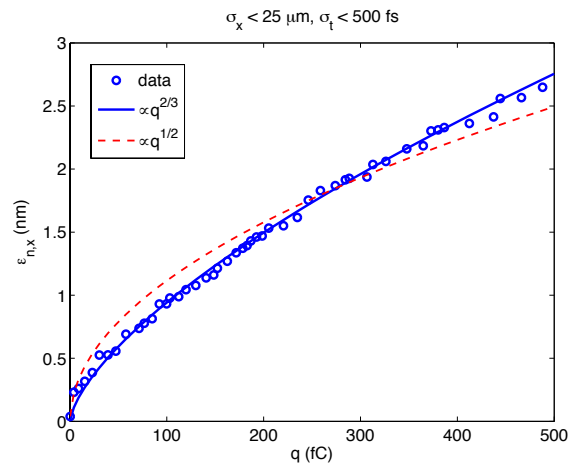


Figure 5: Optimized emittance as a function of bunch charge for NCRF gun.

6 shows the optimal coherence length as a function of the final bunch length, constrained so that $\sigma_x \leq 25 \mu\text{m}$. In particular, the data shows a relative coherence length of $L_{c,x}/\sigma_x \approx 0.07 \text{ nm}/\mu\text{m}$ for a final bunch length of $\sigma_t \approx 5 \text{ fs}$. While the optimizer did not choose solutions at longer bunch lengths in this optimization, using the emittance data in Fig. 3 we estimate the relative coherence length at 30, 100, and 500 fs to be 0.1, 0.2, and 0.3 nm/ μm , respectively. This implies $L_{c,x}(\sigma_t \rightarrow 500 \text{ fs}) \rightarrow 8 \text{ nm}$. Comparing these results, we point out the majority of the improvement comes from using a better cathode MTE.

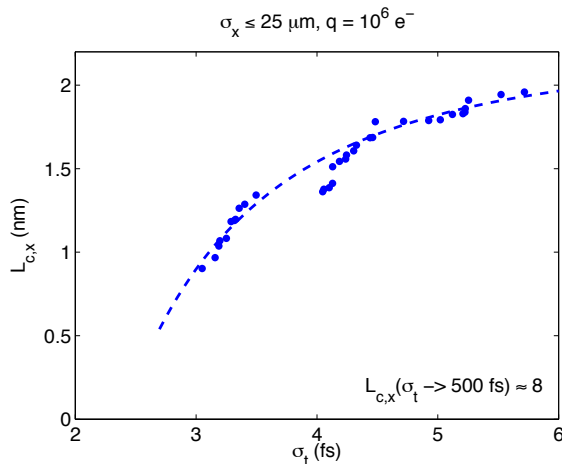


Figure 6: Optimized coherence length as a function of bunch charge for NCRF gun.

CONCLUSION

Optimizations of the emittance as a function of bunch charge demonstrate a $q^{2/3}$ dependence for both beamlines, as anticipated from the basic scaling laws for a long initial beam at the cathode shown here and derived in the literature. Of particular note, emittances as low as 2 - 5 nm were found for final bunch lengths ranging from roughly 500 fs down to 5 fs for a bunch charge of 10^6 electrons in both set-ups (smallest bunch lengths only possible in NCRF beamline).

In addition to computing the optimal emittances as a function of bunch length, optimizations of the coherence length as a function the final bunch length produced coherence lengths suitable for single-shot UED experiments with a final electron beam spot size of $\sigma_x \leq 25$ and bunch charge of 10^6 electrons. Direct optimization of the coherence length as a function of final bunch length produces a roughly order meter long beamlines (cathode to sample) with physically realizable element positions. In particular, direct optimization of the coherence length produced relative coherence lengths

high as 0.07 nm/ μm for a final bunch length of $\sigma_t \approx 5 \text{ fs}$ for the NCRF gun beamline, which shows roughly a factor of two improvement over the cryogun beamline at similar beam parameters. Estimating the relative coherence length using optimal emittance data for final bunch lengths of 30 and 100 fs yields relative coherence lengths of 0.1 and 0.2 nm/ μm , respectively. Based on the $q^{2/3}$ scaling demonstrated in the optimal emittance results for the NCRF gun, we estimate a factor of 4.6 improvement in the relative coherence numbers (0.3, 0.5, and 0.92 nm/ μm respectively) if the bunch charge was reduced to 10^5 electrons in the NCRF beamline.

This grant was funded through NSF, Award No. PHY 1416318.

REFERENCES

- [1] G. Sciaini and R. J. D. Miller, Rep. Prog. Phys. **74**, 096101 (2011).
- [2] R. J. D. Miller, Annu. Rev. Phys. Chem. **65**, 583 (2014).
- [3] B. J. Siwick, J. R. Dwyer, R. E. Jordan, and R. J. D. Miller, J. Appl. Phys. **92**, 1643 (2002).
- [4] C. Gulliford, et al, Phys. Rev. ST Accel. Beams **16**, 073401 (2013).
- [5] C. Gulliford, A. Bartnik, I. Bazarov, B. Dunham, and L. Cultrera, Appl. Phys. Lett. **106**, 094101 (2015).
- [6] A. Bartnik, C. Gulliford, I. Bazarov, L. Cultrera, and B. Dunham, Phys. Rev. ST Accel. Beams **18**, 083401 (2015).
- [7] T. van Oudheusden, E. F. de Jong, S. B. van der Geer, W. P. E. M. O. Öt Root, O. J. Luiten, and B. J. Siwick, J. Appl. Phys. **102**, 093501 (2007).
- [8] T. van Oudheusden, P. L. E. M. Pasmans, S. B. van der Geer, M. J. de Loos, M. J. van der Wiel, and O. J. Luiten, Phys. Rev. Lett. **105**, 264801 (2010).
- [9] R. P. Chatelain, V. R. Morrison, C. Godbout, and B. J. Siwick, Appl. Phys. Lett. **101**, 081901 (2012).
- [10] L. Cultrera, S. Karkare, H. Lee, X. Liu, and I. Bazarov, <http://arxiv.org/abs/1504.05920>.
- [11] J. Maxson, L. Cultrera, C. Gulliford, and I. Bazarov, Appl. Phys. Lett. **106**, 234102 (2015).
- [12] R. Neal, The Stanford Two-Mile Accelerator (W.A. Benjamin, New York, 1968), Vol. 1.
- [13] C. Gulliford, A. Bartnik, I. Bazarov, Phys. Rev. Accel. Beams **19**, 093402 (2016).
- [14] R. K. Li, K. G. Roberts, C. M. Scoby, H. To, and P. Musumeci, Phys. Rev. ST Accel. Beams **15**, 090702 (2012).
- [15] D. Filippetto, P. Musumeci, M. Zolotorev, and G. Stupakov, Phys. Rev. ST Accel. Beams **17**, 024201 (2014).